Insulin-Mimetic Selaginellins from Selaginella tamariscina with Protein Tyrosine Phosphatase 1B (PTP1B) Inhibitory Activity

ARTICLE *in* JOURNAL OF NATURAL PRODUCTS · JANUARY 2015

Impact Factor: 3.8 · DOI: 10.1021/np5005856 · Source: PubMed

7 AUTHORS, INCLUDING:

Zhao Bingtian
Catholic University of Daegu
27 PUBLICATIONS **56** CITATIONS
SEE PROFILE

Md. Yousof Ali
Pukyong National University
17 PUBLICATIONS **50** CITATIONS
SEE PROFILE

JOURNAL OF NATURAL PRODUCTS

Article

pubs.acs.org/jnp

Insulin-Mimetic Selaginellins from *Selaginella tamariscina* with Protein Tyrosine Phosphatase 1B (PTP1B) Inhibitory Activity

Phi-Hung Nguyen,[†] Bing-Tian Zhao,[†] Md Yousof Ali,[‡] Jae-Sue Choi,[‡] Dong-Young Rhyu,[§] Byung-Sun Min,[†] and Mi-Hee Woo*[,†]

[†]College of Pharmacy, Catholic University of Daegu, Gyeongsan 712-702, Republic of Korea

[‡]Department of Food Science & Nutrition, Pukyong National University, Busan 608-737, Republic of Korea

[§]Department of Oriental Medicine Resources, Mokpo National University, Muan 534-729, Republic of Korea

Supporting Information

ABSTRACT: As part of an ongoing search for new antidiabetic agents from medicinal plants, three new (**2**, **4**, and **5**) and two known selaginellin derivatives (**1** and **3**) were isolated from a methanol extract of *Selaginella tamariscina*. The structures of the new compounds were determined by spectroscopic data analysis. All isolates showed strong glucose uptake stimulatory effects in 3T3-L1 adipocyte cells at a concentration of 5 μM. Furthermore, these compounds were found to possess inhibitory effects on PTP1B enzyme activity with IC_{50} values ranging from 4.6 ± 0.1 to 21.6 ± 1.5 μM. Compound **2** showed the greatest potency, with an IC_{50} value of 4.6 ± 0.1 μM, when compared with the positive control (ursolic acid, IC_{50} = 3.5 ± 0.1 μM). Therefore, these selaginellin derivatives may have value as new lead compounds for the development of agents against type 2 diabetes.

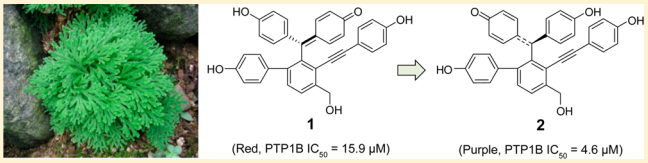

Diabetes mellitus is the world's most prevalent endocrine disease and is characterized by chronic hyperglycemia associated with abnormalities in carbohydrate, fat, and protein metabolism. It is caused by the absence or relative insufficiency of insulin secretion and/or insulin action that leads to the progressive deterioration of glucose tolerance and causes hyperglycemia.[1] Diabetes mellitus is a major and growing public health problem throughout the world, affecting about 171 million people, with the majority having type 2 diabetes.[2] The number of people with diabetes is expected to exceed 300 million globally by 2025.[3a] The American Diabetes Association reported that about 22.3 million people in the United States have diabetes, accounting for 7% of the population.[3b] Thus, great efforts are being made in the search for new therapeutic agents to stem its progress.[4] For some time, insulin was the primary agent available for the treatment of either type 1 or severe type 2 diabetes.[5] Recently, a number of synthetic small molecules, such as zinc(II) complexes and vanadium compounds, have been shown to mimic the action of insulin in cell culture and animal models of diabetes. In addition, many natural products, such as antibiotics (e.g., anisomycin), fungal metabolites (e.g., L-783,281), and plant extracts promote glucose uptake in cells.[6,7] However, clinical tests have shown that none of these compounds or extracts can replace insulin in the treatment of diabetes. Therefore, there is still the need to search for new antidiabetic agents that can mimic the effect of insulin. In addition, the characterization of new insulin-mimetic agents may promote the discovery of new drug targets that further an understanding of the biochemical mechanisms of diabetes and insulin resistance.

Binding of insulin to its receptor results in the phosphorylation of insulin receptor substrates (IRSs), which activates several signaling cascades leading to biological responses such as glucose transport into the cell and glycogen synthesis.[8] Protein tyrosine phosphatases (PTPs), which dephosphorylate the tyrosine residues of proteins, are considered as negative regulators of insulin signaling. Of the various PTPs, protein tyrosine phosphatase 1B (PTP1B) plays a key role in the insulin-dependent signal cascade and has attracted attention as a potential target for the treatment of type 2 diabetes.[9] There are a number of examples in which increased expression of PTP1B decreases the amount of IR tyrosine phosphorylation. PTP1B directly interacts with activated insulin receptor or insulin receptor substrate-1 (IRS-1) to dephosphorylate phosphotyrosine residues, resulting in down-regulation of insulin action.[10] In cell culture tests, overexpression of PTP1B showed a decrease in insulin-stimulated phosphorylation of IR and/or IRS-1, whereas reduction in the level of PTP1B, by antisense oligonucleotides or neutralizing antibodies, augments insulin-initiated signaling.[11] In animal tests, PTP1B knock-down mice showed enhanced insulin sensitivity in glucose and insulin tolerance, indicating that PTP1B is a major factor in the modulation of insulin sensitivity.[12] Interestingly, $PTP1B^{-/-}$ mice are protected against weight gain and have significantly lower triglyceride levels when placed on a high-fat diet. Moreover, increased expression of PTP1B in adipose tissue and muscle of obese humans and rodents is

Received: July 23, 2014
Published: January 6, 2015

DOI: 10.1021/np5005856
J. Nat. Prod. 2015, 78, 34−42

thought to be related to insulin resistance,[13] whereas the increased insulin sensitivity from weight loss is accompanied by reduced PTP1B activity.[14] In addition, PTP1B overexpression in rat primary adipose tissues and 3T3-L1 adipocytes has been shown to decrease insulin-sensitive Glut4 translocation[15] and insulin receptor and IRS-1 phosphorylation,[16] respectively.

As with the insulin signaling pathway, the leptin signaling pathway can be attenuated by PTPs, and there is evidence that PTP1B is also involved in this process. PTP1B was shown subsequently to bind and dephosphorylate JAK2, which is downstream of leptin receptor. Thus, the resistance to diet-induced obesity observed in PTP1B$^{-/-}$ mice is likely associated with increased energy expenditure owing to enhanced leptin sensitivity.[17] Moreover, pretreatment of leptin-resistant rats with a potent and selective PTP1B inhibitor resulted in a marked improvement in leptin-dependent suppression of food intake.[18] Therefore, it has been suggested that compounds that reduce PTP1B activity or expression levels can be used for treating not only type 2 diabetes but also obesity.[8,19] Although there have been a number of reports on the design and development of these compounds,[20] new types of PTP1B inhibitors with suitable pharmacological properties remain to be discovered.

Selaginella, also known as spikemoss, is the only surviving genus within the plant family Selaginellaceae. *Selaginella* includes more than 700 species widely distributed around the globe.[21] Among the genus, *Selaginella tamariscina* (Beauv.) Spring was first recorded by "Shen Nong Ben Cao Jing" (*The Divine Farmer's Materia Medica*) in 2737 B.C. It has been used in oriental medicine to treat inflammation, amenorrhea, dysmenorrhea, metrorrhagia, hematuria, prolapse of the anus, abdominal lumps in women, chronic hepatitis, and hyperglycemia.[22] Moreover, *S. tamariscina* has been reported to lower blood glucose levels and to facilitate the repair of pancreatic islet β-cells injured by alloxan.[23] A number of flavonoids, biflavonoids, lignans, selaginellins, and phenols were reported as chemical constituents of *S. tamariscina*.[24]

As part of an ongoing investigation on the discovery of new antidiabetic agents from medicinal plants, the methanol extract of the aerial parts of *S. tamariscina* was found to increase in vitro glucose uptake in 3T3-L1 adipocytes. Thus, phytochemical investigation of this medicinal plant using chromatographic methods led to the isolation of three new natural products (**2**, **4**, and **5**) and two known selaginellin derivatives. Furthermore, the stimulatory effects of compounds **1**−**5** were evaluated on 2-NBDG uptake in 3T3-L1 adipocyte cells along with their inhibitory effects on PTP1B enzyme activity. In this report, the purification, structural determination, and potential antidiabetic properties of these isolates are discussed.

RESULTS AND DISCUSSION

A bioassay-guided investigation of the methanol extract of the aerial part of *S. tamaricina* has led to the isolation of three new (**2**, **4**, and **5**) and two known (**1** and **3**) selaginellin derivatives as active principles. The known compounds were determined to be selaginellin (**1**) and selaginellin M (**3**) from a comparison of their physical and spectroscopic data (IR, UV, NMR, and MS) with those reported in the literature.[16]

Compound **2** was obtained as a purple, amorphous powder. Its HREIMS showed a molecular ion peak at m/z 512.1626 $[M]^+$ (calcd for m/z 512.1624), consistent with a molecular formula of $C_{34}H_{24}O_5$. The IR spectrum indicated absorption bands for hydroxy group (3394 cm^{-1}), alkynyl (2203 cm^{-1}), unsaturated carboxyl (1680 cm^{-1}), and C−O (1077−1045 cm^{-1}) stretching vibrations. Its UV spectrum showed absorption maxima at 266, 300, 322, and 433 nm, characteristic values for a selaginellin analogue.[16] The assignment of the ^{1}H and ^{13}C NMR data (Tables 1 and 2) was supported by 2D NMR techniques (Supporting Information). In the ^{1}H and ^{13}C NMR spectra of **2**, the typical signals of an alkynyl substituent at δ_C 84.4 and 101.1, an AB spin system at δ_H 7.38 and 7.74 (each 1H, d, J = 8.0 Hz) for the *ortho*-tetrasubstituted A-ring, four AA′BB′ systems [δ_H 6.97 and 6.62 (each 2H, dd, J = 2.0, 8.8 Hz); δ_H 6.87 and 6.51 (each 2H, dd, J = 2.0, 8.4 Hz)] for the *para*-substituted B- and E-rings, and the symmetrical signals at δ_H 7.18 and 6.46 (each 4H, dd, J = 2.0, 8.8 Hz) for the C- and D-rings were apparent. The alkynyl group was connected to the B-ring based on HMBC correlations between H-29 and H-33 and C-28. The linkage between the C-ring and the D-ring was located at C-7 (170.2), as demonstrated by the HMBC cross-peaks of H-3, H-5/C-7 and H-8, H-12/C-7 (Figure 1). The E-ring was connected to the A-ring at C-18, as supported by the HMBC correlations between H-20/H-24 and C-18 and H-17/C-18 and C-25. Hence, C-19 (142.5) in the A-ring was the only position left for C-7. The bond between C-7 and C-19 formed a chiral axis for steric hindrance. In the ^{1}H NMR spectra of both compounds **1** and **2**, extensive delocalization took place in rings C and D, which caused these substances to become racemic.[16] The delocalization of the π-electrons resulted in rings C and D being chemically equivalent,[17] so the signals assigned for H-3, H-5, H-8, and H-12 appeared at δ_H 7.18 (4H, dd, J = 2.0, 8.8 Hz), and also the signals assigned for H-2, H-6, H-9, and H-11 occurred at δ_H 6.46 (4H, dd, J = 2.0, 8.8 Hz). Therefore, in the NOESY NMR spectra of these compounds, the correlations between the protons of ring C and the protons of ring B and between the protons of ring D and those of ring B appeared similarly, and the correlations of the protons of ring C and ring D with the protons of ring E were also identical.

All of the above structural features for compound **2** were identical with those of selaginellin (**1**).[16] However, the physical and chemical properties of compound **2** were found to be somewhat different from those of compound **1**. Indeed, the analytical HPLC profile of a mixture of compounds **1** and **2**

DOI: 10.1021/np5005856
J. Nat. Prod. 2015, 78, 34−42

Table 1. ^{1}H NMR Spectroscopic Data (400 MHz, CD_3OD) for Isolated Compounds 1−5

	1	2	3	4[a]	5
position	δ_H (J in Hz)	δ_H (J in Hz)	δ_H (J in Hz)	δ_H (J in Hz)	δ_H (J in Hz)
2	6.51 (br d, 8.8)	6.46 (dd, 2.0, 8.8)	6.47 (dd, 2.4, 10.0)	6.66 (dd, 2.0, 8.8)	6.58 (dd, 2.0, 8.4)
3	7.14 (br d, 8.8)	7.18 (dd, 2.0, 8.8)	7.48 (dd, 2.8, 10.0)	7.15 (dd, 2.0, 8.8)	7.10 (dd, 2.0, 8.4)
4					
5	7.14 (br d, 8.8)	7.18 (dd, 2.0, 8.8)	7.59 (dd, 2.8, 10.0)	7.15 (dd, 2.0, 8.8)	7.10 (dd, 2.0, 8.4)
6	6.51 (br d, 8.8)	6.46 (dd, 2.0, 8.8)	6.44 (dd, 2.4, 10.0)	6.66 (dd, 2.0, 8.8)	6.58 (dd, 2.0, 8.4)
7					
8	7.14 (br d, 8.8)	7.18 (dd, 2.0, 8.8)	6.77 (dd, 2.0, 8.8)	7.15 (dd, 2.0, 8.8)	7.10 (dd, 2.0, 8.4)
9	6.51 (br d, 8.8)	6.46 (dd, 2.0, 8.8)	6.75 (dd, 2.0, 8.8)	6.66 (dd, 2.0, 8.8)	6.58 (dd, 2.0, 8.4)
10					
11	6.51 (br d, 8.8)	6.46 (dd, 2.0, 8.8)	6.75 (dd, 2.0, 8.8)	6.66 (dd, 2.0, 8.8)	6.58 (dd, 2.0, 8.4)
12	7.14 (br d, 8.8)	7.18 (dd, 2.0, 8.8)	6.77 (dd, 2.0, 8.8)	7.15 (dd, 2.0, 8.8)	7.10 (dd, 2.0, 8.4)
13					
14					
15					
16	7.70 (d, 8.0)	7.74 (d, 8.0)	7.72 (d, 7.6)	7.59 (d, 8.0)	7.42 (d, 7.6)
17	7.33 (d, 8.0)	7.38 (d, 8.0)	7.34 (d, 7.6)	7.75 (d, 8.0)	7.67 (d, 7.6)
18					
19					
20	6.76 (br d, 8.4)	6.87 (dd, 2.0, 8.4)	6.85 (dd, 2.0, 8.8)	7.67 (d, 8.0)	7.61 (d, 8.4)
21	6.53 (br d, 8.4)	6.51 (dd, 2.0, 8.4)	6.54 (dd, 2.0, 8.8)	6.84 (dd, 2.0, 8.0)	6.78 (dd, 2.0, 8.4)
22					
23	6.53 (br d, 8.4)	6.51 (dd, 2.0, 8.4)	6.54 (dd, 2.0, 8.8)	6.78 (d, 2.0)	6.71 (d, 2.0)
24	6.76 (br d, 8.4)	6.87 (dd, 2.0, 8.4)	6.85 (dd, 2.0, 8.8)		
25					
26	4.94 (s)	4.94 (s)	4.96 (s)	4.82 (s)	4.63 (s)
27					
28					
29	6.98 (br d, 8.8)	6.97 (dd, 2.0, 8.8)	6.99 (dd, 2.0, 8.8)	6.98 (dd, 2.0, 8.8)	6.87 (dd, 2.0, 8.8)
30	6.62 (br d, 8.8)	6.62 (dd, 2.0, 8.8)	6.63 (dd, 2.0, 8.8)	6.80 (dd, 2.0, 8.8)	6.69 (dd, 2.0, 8.8)
31					
32	6.62 (br d, 8.8)	6.62 (dd, 2.0, 8.8)	6.63 (dd, 2.0, 8.8)	6.80 (dd, 2.0, 8.8)	6.69 (dd, 2.0, 8.8)
33	6.98 (br d, 8.8)	6.97 (dd, 2.0, 8.8)	6.99 (dd, 2.0, 8.8)	6.98 (dd, 2.0, 8.8)	6.87 (dd, 2.0, 8.8)
34					
$-OCH_3$			3.77 (s)		3.43 (s)

[a]Measured in acetone-d_6.

showed that compound **2** had a longer retention time (t_R = 30.1 min) on a C_{18} column than compound **1** (t_R = 26.5 min) (see Supporting Information). Furthermore, compound **2** was obtained as a purple powder, while selaginellin (**1**) was isolated as a red natural pigment.[16] Thus, the color changes of compounds **1** and **2** were considered in more detail, and a plausible mechanism is shown in Scheme 1. The pH ranges for the color change of compound **1** were at 7.5−8.0 (red to purple) and 1.5−1 (red to pink). Noticeably, the range (7.5−8.0) is very close to pH = 7.0 (neutral). Thus, it may be predicted that compound **2** is a biosynthetic derivative of **1** via tautomerism (Scheme 1).[17] Consequently, an acetoxy derivative (**2a**) was synthesized by base-catalyzed acetylation as evidence of the presence of **2**. Compound **2a** was obtained as a yellow material with a molecular formula of $C_{42}H_{32}O_9$ as determined by the molecular ion m/z 680 (100%) and other peaks at 638 (83%), 596 (60%), 554 (37%), and 512 (13%) in its LREIMS (see Supporting Information). Moreover, compound **2** showed negative Cotton effects at 206 and 214 nm and positive Cotton effects at 210 and 220 nm in its CD spectrum, while compound **1** displayed the opposite, with positive Cotton effects at 206 and 214 nm and negative Cotton effects at 210 and 222 nm (Supporting Information). In addition, compound **1** (R) gave a negative specific rotation value of −13.0 (c 0.5, MeOH), while compound **2** exhibited a positive specific rotation value of +105 (c 0.1, MeOH), revealing an S-configuration.[16−18] Thus, compound **2** (selariscinin A) was established as (*S*)-4-[(4′-hydroxy-4-(hydroxymethyl)-3-((4-hydroxyphenyl)ethynyl)biphenyl-2-yl)(4-hydroxyphenyl)methylene]-2,5-cyclohexadien-1-one, which is a new natural product.

Compound **4** was purified as a greenish-pink amorphous powder. The molecular formula was determined as $C_{34}H_{26}O_7$ from the ^{13}C NMR data and the molecular ion peak at m/z 546.1683 $[M]^+$ (calcd m/z 546.1679) obtained by HREIMS. UV bands at λ_{max} 265, 300, 322, and 416 nm suggested the presence of a selaginellin derivative.[16,17] The IR spectrum indicated the presence of OH (3386 cm^{-1}), C−H (2943, 2853 cm^{-1}), C≡C (2198 cm^{-1}), C═C (1641, 1599 cm^{-1}), C−H (1453, 1379 cm^{-1}), and C−O (1078, 1041 cm^{-1}) functionalities. A negative specific rotation value of −4.7 (c 0.25, MeOH) was observed for compound **4**. The ^{1}H and ^{13}C NMR spectra of this isolate displayed an AB spin system (δ_H 7.59 and 7.75, each 1H, d, J = 8.0 Hz) for the *ortho*-tetrasubstituted A-ring, an AA′BB′ system (δ_H 6.98 and 6.80, each 2H, dd, J = 2.0, 8.8 Hz) for the *para*-substituted B-ring, and another two symmetrical AA′BB′ spin systems for the respective *para*-substituted C- and D-rings [δ_H 7.15 and 6.66 (each 4H, dd, J = 2.0, 8.8 Hz)]. The corresponding carbons resonating at δ_C 156.9 (C-1/-10), 115.2 (C-2, -6, -9, -11), 131.2 (C-3, -5, -8, -12), and 134.9 (C-4 and C-13) further supported this observation. Moreover, an ABX spin system was present at δ_H 7.67 (1H, d, J = 8.0 Hz, H-20), 6.84 (1H, dd, J = 2.0, 8.0 Hz, H-21), and 6.78 (1H, d, J = 2.0 Hz, H-23) for the E-ring. In addition, the typical signals of an alkynyl band at δ_C 85.3 and 102.1 were also found. All of these assignments were confirmed by ^{1}H−^{1}H gCOSY and ^{1}H−^{13}C gHMQC experiments (Figure 1 and Supporting Information). In the HMBC spectrum, the correlations between H-29 and C-31/33/34 and C-28 in addition to H-30 and C-31/32/34 indicated that the C≡C bond is connected to ring B. Ring E was shown to be connected to C-18 via correlations between H-17 and C-18 and C-25 as well as H-20 and C-18 and C-25, with H-23 correlated to C-21 (115.6), C-22 (158.8), C-24 (157.3), and C-25 (131.8), respectively. The remaining two symmetrical *para*-substituted C- and D-rings were connected to ring A through a C-7−C-19 symmetrical axis, as evidenced by correlations between the oxygenated C-7 (65.8) and H-3, H-5, H-8, and H-12 (Figure 1). The linkage position of the hydroxymethyl group [δ_H 4.82 (2H, s, H-26) and δ_C 63.3 (C-26)] to C-15 in ring A was established by HMBC cross-peaks of H-26/C-14, H-26/C-15,

DOI: 10.1021/np5005856
J. Nat. Prod. 2015, 78, 34−42

Table 2. ^{13}C NMR Spectroscopic Data (100 MHz, CD_3OD) for Compounds 1−5

	1	2	3	4[a]	5
position	δ_C, type	δ_C, type	δ_C, type	δ_C, type	δ_C, type
1	165.6, C	181.7, C	189.4, C	156.9, C	157.1, C
2	122.3, CH	123.3, CH	128.6, CH	115.2, CH	115.4, CH
3	138.9, CH	140.6, CH	142.4, CH	131.2, CH	131.5, CH
4	131.9, C	131.6, C	131.8, C	134.9, C	135.3, C
5	138.9, CH	140.6, CH	141.7, CH	131.2, CH	131.5, CH
6	122.3, CH	123.3, CH	129.0, CH	115.2, CH	115.4, CH
7	165.6, C	170.2, C	164.6, C	65.8, C	66.3, C
8	138.9, CH	140.6, CH	134.2, CH	131.2, CH	131.5, CH
9	122.3, CH	128.5, CH	114.7, CH	115.2, CH	115.4, CH
10	165.6, C	181.7, C	163.1, C	156.9, C	157.1, C
11	122.3, CH	128.5, CH	114.7, CH	115.2, CH	115.4, CH
12	138.9, CH	140.6, CH	134.2, CH	131.2, CH	131.5, CH
13	131.9, C	131.6, C	132.6, C	134.9, C	135.3, C
14	123.9, C	124.4, C	123.8, C	119.7, C	122.1, C
15	143.0, C	142.8, C	143.1, C	143.1, C	138.5, C
16	128.9, CH	128.8, CH	128.7, CH	126.7, CH	129.1, CH
17	131.1, CH	130.7, CH	131.0, CH	119.5, CH	119.5, CH
18	143.6, C	143.9, C	143.5, C	140.7, C	142.3, C
19	142.4, C	142.5, C	143.0, C	152.9, C	153.9, C
20	131.2, CH	130.9, CH	131.2, CH	121.5, CH	121.9, CH
21	115.9, CH	115.8, CH	115.9, CH	115.6, CH	115.9, CH
22	158.0, C	158.0, C	158.1, C	158.8, C	159.6, C
23	115.9, CH	115.8, CH	115.9, CH	113.4, CH	113.6, CH
24	131.2, CH	130.9, CH	131.2, CH	157.3, C	157.8, C
25	133.1, C	133.1, C	132.7, C	131.8, C	132.1, C
26	63.7, CH_2	63.6, C	63.7, CH_2	63.3, CH_2	74.4, CH_2
27	84.7, C	84.4, C	84.7, C	85.3, C	85.7, C
28	100.7, C	101.1, C	100.7, C	102.1, C	102.5, C
29	134.2, CH	134.3, CH	134.7, CH	133.5, CH	133.9, CH
30	116.5, CH	116.8, CH	116.5, CH	116.5, CH	116.7, CH
31	159.6, C	160.5, C	159.7, C	158.8, C	159.4, C
32	116.5, CH	116.8, CH	116.5, CH	116.5, CH	116.7, CH
33	134.2, CH	134.3, CH	134.7, CH	133.5, CH	133.9, CH
34	114.6, C	114.1, C	114.6, C	115.5, C	115.9, C
$-OCH_3$			56.1, CH_3		58.9, CH_3

[a]Measured in acetone-d_6.

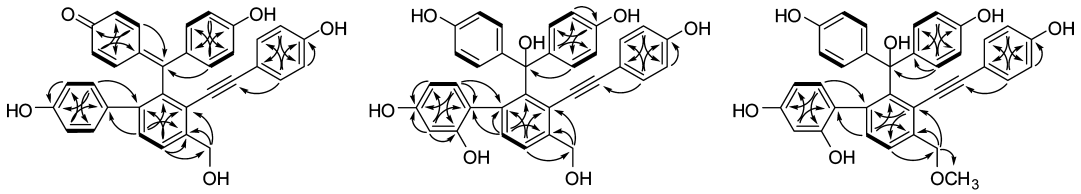

Figure 1. $^1H-^1H$ COSY (bold lines) and $^1H-^{13}C$ key HMBC correlations (arrows) for the new compounds, selariscinins A (2), B (4), and C (5).

and H-16/C-26. On the basis of the above evidence, compound 4 (selariscinin B) was thus characterized as 2-(hydroxybis(4-hydroxyphenyl)methyl)-3-((4-hydroxyphenyl)ethynyl)-4-(hydroxymethyl)biphenyl-2′,4′-diol and is representative of a new skeleton for the selaginellins.

The physicochemical and spectroscopic (^1H, ^{13}C, gCOSY, gHMQC, and gHMBC) data of compound 5 were identical with those of 4 (Figure 1, Tables 1 and 2, and Supporting Information) except for an additional methoxy group [δ_H 3.43 (3H, s) and δ_C 58.9] evident in compound 5. This methoxy group could be connected to C-15 of the A-ring through an oxygenated methylene moiety [δ_H 4.63 (2H, s, H-26) and δ_C 74.4 (C-26)], according to the HMBC correlations between protons of the methoxy group (δ_H 3.43) and C-26 (74.4), between H-26 and C-14 (122.1) and C-15 (138.5), and between H-16 (7.42, 1H, d, J = 7.6 Hz) and C-26. Furthermore, an AB spin system (δ_H 7.42 and 7.67, each 1H, d, J = 7.6 Hz) for the *ortho*-tetrasubstituted A-ring, an AA′BB′ system [δ_H 6.87 and 6.69, each 2H, dd, J = 2.0, 8.8 Hz] for the *para*-substituted B-ring, two symmetrical AA′BB′ spin systems for the respective *para*-substituted C- and D-rings [δ_H 7.10 and 6.58, each 4H, dd, J = 2.0, 8.4 Hz], and an ABX spin system [δ_H 7.61 (1H, d, J = 8.4 Hz, H-20), 6.78 (1H, dd, J = 2.0, 8.4 Hz, H-21), and 6.71 (1H, d, J = 2.0 Hz, H-23)] for the E-ring, as well

DOI: 10.1021/np5005856
J. Nat. Prod. 2015, 78, 34−42

Scheme 1. Tautomerism of Compounds 1 and 2 (⇀) and the Synthesis of 2a, and Plausible Mechanisms for the Color Changes of Compounds 1−4 (→)

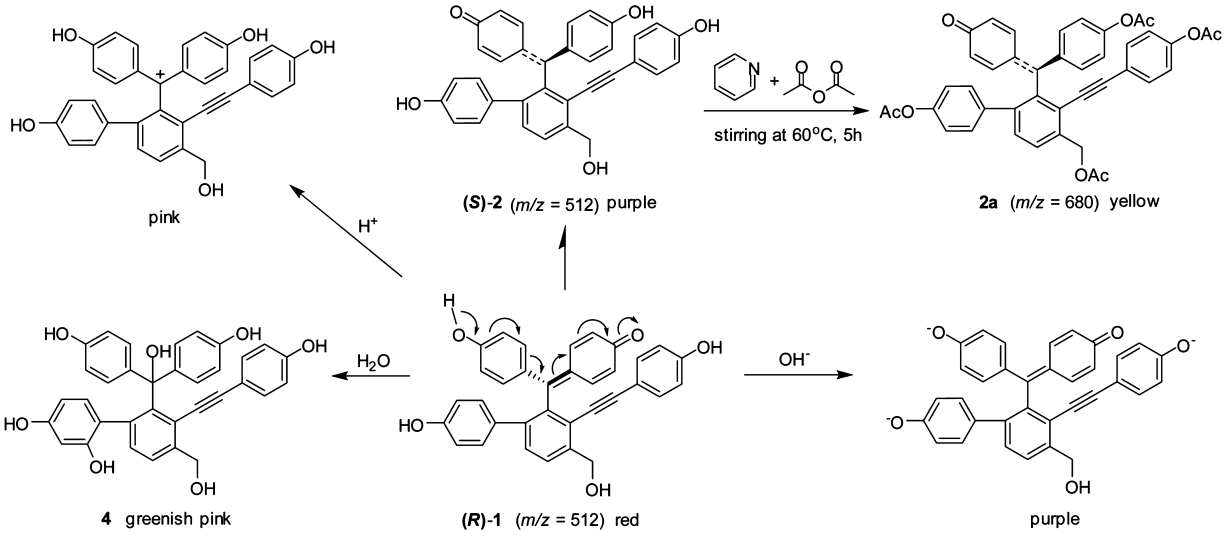

as the typical signals of an alkynyl band (δ_C 85.7 and 102.5), were also observed. The assignment and arrangement of these rings were established based on 2D NMR spectroscopic data analysis (Figure 1). The substitution of the hydroxy group at C-7 led to C-7 being shifted upfield (66.3) and C-19 downfield (153.9). In addition, the HREIMS data of compound **5** (*m*/*z* 560.1839 $[M]^+$, calcd for $C_{35}H_{28}O_7$, 560.1835) revealed an additional methyl group when compared with that of compound **4** (*m*/*z* 546.1683 $[M]^+$, calcd for $C_{34}H_{26}O_7$). A negative specific rotation value at −82.1 (*c* 0.1, MeOH) was observed for compound **5**. From the above data, the new compound **5** (selariscinin C) was thus identified as 2-(hydroxybis(4-hydroxyphenyl)methyl)-3-((4-hydroxyphenyl)-ethynyl)-4-(methoxymethyl)biphenyl-2′,4′-diol.

Selaginellins are a group of phenols based on a chemical scaffold found only to date in the genus *Selaginella*. Selaginellin (**1**), the first member of this compound class, was isolated as a racemic mixture, containing a *p*-quinone methide unit and an alkynylphenol moiety, in *S. sinensis*.[16−18] To date, about 14 additional compounds structurally related to selaginellin have been identified from *Selaginella* species.[16−18] In the present study, compounds **4** and **5** were obtained as new skeleton of selaginellins bearing a hydroxy group at C-7. The *p*-quinone methide unit at C-1 of selaginellin was also hydrogenated. Under acidic conditions, the color is changed from red (selaginellin **1**) to pink (compound **4**), and it may be assumed that acid-catalyzed hydration may occur; then the addition of an aqueous molecule to compound **1** is reached at C-7 and C-1 (Scheme 1) to form a symmetrical partial structure of the C- and D-rings through the C-7−C-19 axis in compounds **4** and **5**. All of the isolated compounds **1**−**5** were obtained with a purity grade of more than 98% according to their HPLC analysis patterns (Supporting Information).

2-NBDG has been reported as a useful fluorescent-tagged glucose probe for discovering insulin mimetic compounds.[22] Thus, the stimulatory effects of compounds **1**−**5** were further evaluated on glucose uptake using 2-NBDG in 3T3-L1 adipocyte cells.[23] At a concentration of 5 μM, compounds **1**−**5** significantly stimulated 2-NBDG uptake by 1.2 ± 0.1-, 1.3 ± 0.1-, 1.4 ± 0.1-, 1.1 ± 0.2-, and 1.2 ± 0.1-fold induction as compared with the control (DMSO), respectively (Figure 2).

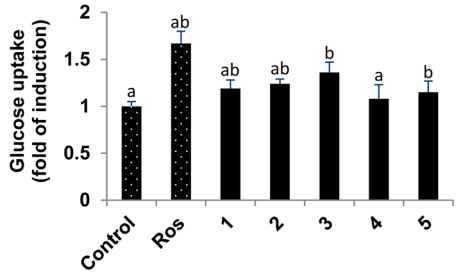

Figure 2. Stimulatory effects of the isolated compounds (**1**−**5**) and the positive control (Ros: rosiglitazone) on glucose uptake in 3T3-L1 adipocyte cells. Confluent 3T3-L1 preadipocytes were differentiated into adipocytes for 8 days (from day 0 to day 8). Fully differentiated 3T3-L1 adipocytes were treated with 5 μM of each compound and rosiglitazone followed by treatment with 2-NBDG, a fluorescent derivative of glucose used as a glucose analogue for 30 min. Glucose uptake was measured using a fluorescence reader. Bars with different letters are significantly different at $p < 0.05$ by Duncan's multi-comparison tests.

In this assay, the positive control (rosiglitazone) showed an induction of 1.7 ± 0.1. Selaginellin M (**3**), with a methoxy group at C-10, showed a more potent effect than selaginellin (**1**). Similarly, compound **5**, with a methoxy group at C-26, also possessed more potency than compound **4**. The isolated compounds **1**−**5** did not show cytotoxicity to the cells even at concentrations at 50 μM, except for compound **3**, which displayed 54% inhibition (Supporting Information).

GLUT4 glucose transport translocation is essential for inducible glucose uptake into the plasma membrane in muscle and adipocyte cells. This process depends mainly on the regulation of two physiological pathways: the AMP-activated protein kinase (AMPK) pathway and the insulin signaling pathway.[24a] In the insulin signaling pathway, binding of insulin to the insulin receptor on adipocytes and muscle cells triggers the recruitment and phosphorylation of insulin receptor substrate, which forms a docking site for PI3K at the membrane. When docked, PI3K activates phosphoinositide-dependent protein kinase 1 (PDK1), which in turn mediates the phosphorylation of both Akt (also known as protein kinase B) at Thr^{308} and ribosomal protein 70 kDa S6 kinase 1

DOI: 10.1021/np5005856
J. Nat. Prod. 2015, 78, 34−42

($p70^{s6k}$).[24] Thus, activated Akt facilitates glucose uptake in adipocytes and muscle cells by allowing the translocation of GLUT4, the insulin-responsive isoform of the glucose transporter located in intracellular storage vesicles, to the plasma membrane.[24] As a negative regulator, PTP1B dephosphorylates IR and IRS in the case of insulin signaling and also tyrosine kinase JAK2 (Janus kinase 2) in the leptin signaling pathway.[25] Therefore, inhibition of the activity or the expression level of PTP1B can facilitate the insulin signaling pathway, leading to an increase in glucose uptake in adipocytes. In this regard, the inhibitory effects of compounds **1**−**5** on the PTP1B enzyme were measured using ursolic acid[26] and a synthetic (1,3,4)-oxadiazole derivative (NCE-9)[27] as positive controls (Table 3).

Table 3. Inhibitory Effects of Isolated Compounds 1−5 on PTP1B Enzyme Activity

compound	inhibitory effect (IC_{50}, μM)[a]	K_i value (μM)	inhibition type
1	15.9 ± 0.6	13.9 ± 0.8	mixed-competitive
2	4.6 ± 0.1	3.0 ± 0.2	mixed-competitive
3	11.5 ± 0.2	8.9 ± 0.6	mixed-competitive
4	21.6 ± 1.5	10.3 ± 2.2	noncompetitive
5	19.4 ± 0.4	15.1 ± 1.9	uncompetitive
ursolic acid[b]	3.5 ± 0.1	−[c]	−
NCE-9[b]	0.7 ± 0.1	−	−

[a]Results are expressed as IC_{50} values (μM), determined by regression analysis and expressed as the means ± SD of three replicates. [b]Positive control (NCE-9: 5-biphenyl-4-yl-[1,3,4]oxadiazole-2-carboxylic acid). [c]Data not determined.

Among the isolates, compound **2** exhibited equivalent activity (IC_{50} value of 4.6 ± 0.1 μM) to the positive control, ursolic acid (IC_{50} = 3.5 ± 0.1 μM). A kinetic study showed that the inhibition modes of compounds **1**−**3**, as determined using Lineweaver−Burk (Figures 3A and S10 in the Supporting Information) and Dixon plots (Figures 3B and S11 in the Supporting Information), were mixtures of inhibition types. However, both experiments showed that compound **4** exhibited noncompetitive inhibition because the V_{max} values decreased with concentration without changing the K_m for the substrate, and the lines intersected at a value of 1/[S] under zero on the *x*-axis (at 1/(intensity/min) = 0) (Figures S10 and S11, Supporting Information). In contrast, increasing the substrate concentrations resulted in a series of lines that did not intersect on the *y*-axis in the Lineweaver−Burk plot and the *x*-axis in Dixon plots, but paralleled each other, confirming that compound **5** shows uncompetitive inhibition.

Similar structure−activity relationships were observed in PTP1B and 2-NBDG assays for the isolated compounds **1**−**5**. Two selaginellin isomers (**1** and **2**) and the 10-methoxylated selaginellin M (**3**) possessed stronger inhibitory effects on PTP1B enzyme activity than 1,7-dihydroxylated forms (**4** and **5**) (Table 3 and Figure 2). Compounds with a methoxy group in their structure displayed more potent activity in both the PTP1B and 2-NBDG assay than the nonmethoxylated analogues. Thus, it is suggested that the attachment of additional methoxy group may result in an inhibitory effect on the PTP1B enzyme activity and a stimulatory effect on 2-NBDG uptake of these selaginellins.

S. tamariscina has been reported to possess various biological properties such as cytotoxic, antihyperglycemic, antimicrobial, antifungal, anti-inflammatory, and antidiabetic activity.[16,18,28] Compounds **1**−**5** from *S. tamariscina* not only showed stimulatory potency on 2-NBDG uptake but also showed potent inhibitory effects on PTP1B enzyme activity, which suggested the potential of the isolates as insulin mimetics for developing antidiabetes agents. The results reveal a molecular mechanism for the potential beneficial effects of selaginellins on type-2 diabetes and obesity. Further investigation and optimization of these derivatives may enable the preparation of new insulin mimics with potential application in the treatment of type-2 diabetes. The 2-NBDG uptake stimulatory and PTP1B inhibitory effects by the selaginellins have not been previously reported. Further confirmation of the antidiabetes effects of these natural products and evaluation of their in vivo efficacy in a diabetic model are necessary.

EXPERIMENTAL SECTION

General Experimental Procedures. The specific rotations were determined on a JASCO DIP-1000 digital polarimeter (JASCO Corp., Tokyo, Japan) using a 100 mm glass microcell. UV spectra were recorded in MeOH using a Shimadzu UV spectrometer (Shimadzu Corp., Kyoto, Japan). IR spectra (KBr) were recorded on a Nicolet 6700 FT-IR spectrometer (Thermo Electron Corp., Tokyo, Japan). The NMR spectra were recorded in methanol-d_4 (CD_3OD) on a Varian Oxford-AS 400 MHz instrument (Palo Alto, CA, USA), with TMS as the internal standard, at the Department of Pharmacy, Catholic University of Daegu, Korea. All mass spectrometric experiments were performed on a Quattro II mass spectrometer at Korea Basic Science Institute Daegu Center (KBSC, Daegu, Korea). Silica gel (63−200 μm particle size) and RP-C_{18} (40−63 μm particle size) for column chromatography were from Merck (Darmstadt, Germany). Thin-layer chromatography (TLC) was carried out on precoated Merck silica gel 60 F_{254} and RP-C_{18} F_{254} plates from Merck. HPLC was carried out using a Gilson system (Middleton, WI, USA) with a UV detector and an Optima Pak C_{18} column (10 × 250 mm, 10 μm particle size, RS Tech Corporation, Seoul, Korea). HPLC solvents were obtained from Fisher Scientific Korea Ltd. (Seoul, Korea). All other reagents were of the highest analytical grade.

Plant Material. The aerial parts of *Selaginella tamariscina* were purchased from Yeongcheon market, Gyeongbuk, Republic of Korea, in January 2010. The sample was authenticated by one of the authors (B.S.M.). A voucher specimen (CUDP 2010-01) was deposited in the herbarium (CUD) of College of Pharmacy, Catholic University of Daegu, Korea.

Extraction and Isolation. The aerial parts of *S. tamariscina* (1.0 kg) were extracted with methanol (4 × 5 L) using sonication at 45 °C for 10 h. The methanol extract was dried under reduced pressure; then a 150 g aliquot was suspended in H_2O (1.0 L) and partitioned successively with CH_2Cl_2 (1 L × 4, 37.0 g), EtOAc (1 L × 4, 14.8 g), *n*-BuOH (1 L × 4, 65.0 g), and H_2O. The CH_2Cl_2-, EtOAc-, *n*-BuOH-, and H_2O-soluble layers were investigated for their 2-NBDG uptake stimulatory effect in 3T3-L1 adipocyte cells. Among these, the EtOAc fraction demonstrated the most potent activity (Supporting Information). Thus, this fraction (14.5 g) was subjected to silica gel column chromatography (6.0 × 60 cm; 63−200 μm particle size), using a gradient solvent system of CH_2Cl_2−MeOH (10:1 → 0:1), to yield five combined fractions (ST.1 to ST.5) according to their TLC profiles. These fractions were assayed for their 2-NBDG uptake effect (Supporting Information). Fraction ST.2 was subjected to C_{18} reversed-phase (RP-18) column chromatography (3.5 × 25 cm; 40−63 μm particle size) and eluted with MeOH−H_2O (from 65:35 to 100:0, 1 L for each step) to afford five subfractions (ST.2-1 to ST.2-5). Subfraction ST.2-2 was further purified by using a preparative Gilson HPLC system [RS Tech Optima Pak C_{18} column (10 × 250 mm, 10 μm particle size); mobile phase MeCN−H_2O containing 0.1% formic acid (0−30 min: 38% MeCN, 30−33 min: 38−100% MeCN, 33−41

DOI: 10.1021/np5005856
J. Nat. Prod. 2015, 78, 34−42

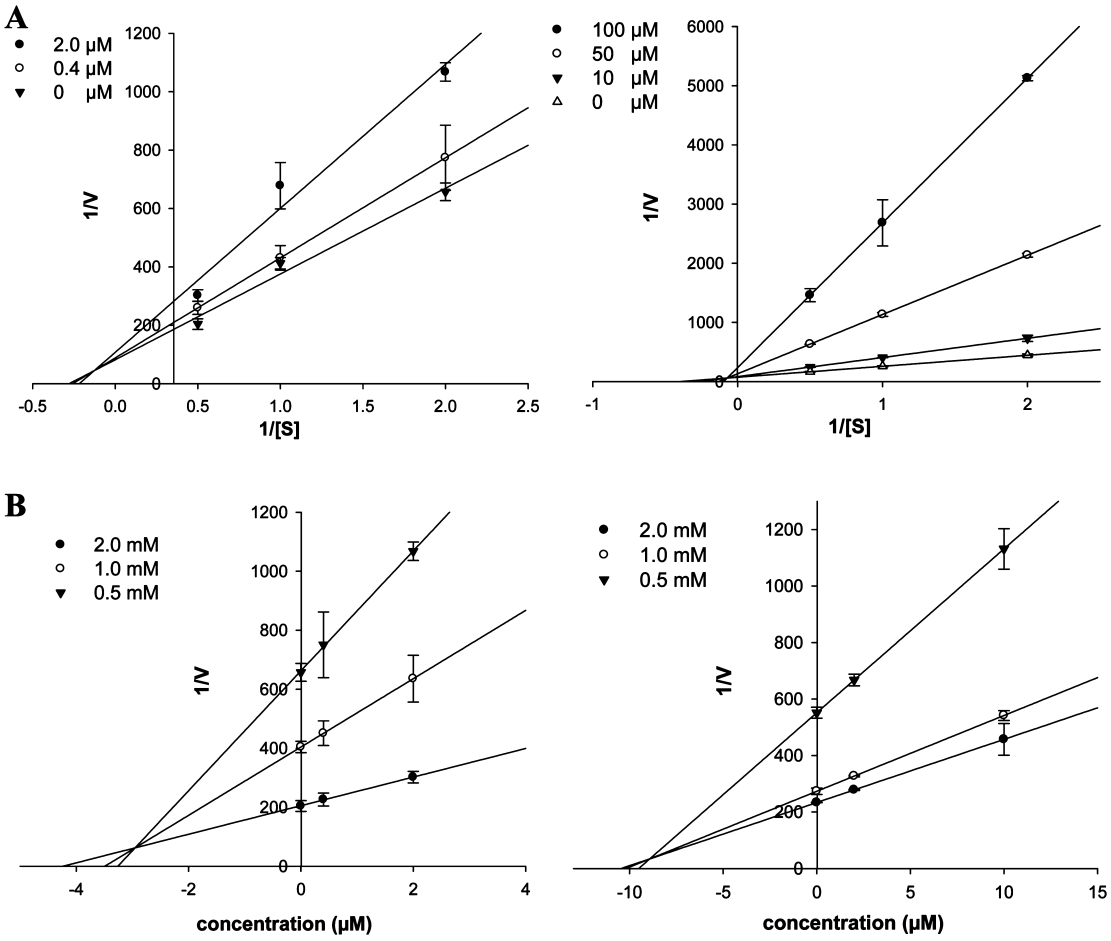

Figure 3. Graphical determination of inhibition type for the isolated compounds **2** and **3**. (A) Lineweaver−Burk plots for the inhibition of isolated compounds **2** and **3** on the PTP1B-catalyzed hydrolysis of *p*-NPP. (B) Dixon plots for isolated compounds **2** and **3** used for determining the inhibition constant K_i. K_i values were determined from the negative *x*-axis value at the point of the intersection of the three lines. Data are expressed as the mean reciprocal of initial velocity for $n = 3$ replicates at each substrate concentration.

min: 100% MeCN, 41−43 min: 100−38% MeCN, 43−45 min: 38% MeCN); UV detection at 225 nm] to give compound **4** (4.4 mg, t_R 20.7 min). Further purification of subfraction ST.2-4 by HPLC using an isocratic solvent system of 64% MeOH in H_2O containing 0.1% formic acid, over 40 min with UV detection at 225 nm, led to the isolation of compounds **3** (16.3 mg, t_R = 26.5 min) and **5** (2.8 mg, t_R = 30.2 min), respectively. Fraction ST.4 was also subjected to C_{18} reversed-phase (RP-18) column chromatography (3.0 × 20 cm; 40−63 μm particle size) and eluted with MeOH−H_2O (from 5:5 to 5:1), resulting in the isolation of compounds **1** (115.6 mg) and **2** (65.0 mg), respectively.

Selariscinin A (2): purple, amorphous powder (acetone); $[\alpha]_D^{25}$ +105 (*c* 0.5, MeOH); UV (*c* 0.02, MeOH) λ_{max} (log ε) 205 (4.68), 266 (4.38), 300 (4.38), 322 (4.26), 433 (4.12) nm; IR ν_{max} (KBr) 3394 (OH), 2943 (C−H), 2203 (C≡C), 1641, 1631 (C═C), 1381 (C−H), 1077, 1045 (C−O) cm^{-1}; CD (MeOH) $[\theta]_{206}$ −98.3, $[\theta]_{210}$ +19.5, $[\theta]_{214}$ −13.6, $[\theta]_{220}$ +4.5; ^1H (400 MHz) and ^{13}C (100 MHz) NMR data in MeOH-d_4, see Tables 1 and 2; HREIMS *m*/*z* 512.1626 $[M]^+$ (calcd for $C_{34}H_{24}O_5$, 512.1624).

Selariscinin B (4): greenish-pink, amorphous powder; $[\alpha]_D^{25}$ −4.7 (*c* 0.25, MeOH); UV (*c* 0.01, MeOH) λ_{max} (log ε) 205 (4.99), 265 (4.77), 300 (4.71), 322 (4.57), 416 (4.44) nm; IR ν_{max} (KBr) 3386 (OH), 2943 (C−H stretching), 2205−2198 (C≡C), 1641, 1599 (C═C), 1453, 1379 (C−H bending), 1166, 1078, 1041 (C−O), 887, 669 cm^{-1}; ^1H (400 MHz) and ^{13}C (100 MHz) NMR data in acetone-d_6, see Tables 1 and 2; HREIMS *m*/*z* 546.1683 $[M]^+$ (calcd for $C_{34}H_{26}O_7$, 546.1679).

Selariscinin C (5): pale yellow, amorphous powder; $[\alpha]_D^{25}$ −82.1 (*c* 0.1, MeOH); UV (*c* 0.005, MeOH) λ_{max} (log ε) 205 (4.68), 266 (4.31), 300 (4.34), 322 (4.22), 433 (4.10) nm; IR ν_{max} (KBr) 3400 (OH), 2201 (C≡C), 1641, 1622 (C═C), 1468, 1374 (C−H bending), 1154, 996 (C−O) cm^{-1}; ^1H (400 MHz) and ^{13}C (100 MHz) NMR data in MeOH-d_4, see Tables 1 and 2; HREIMS *m*/*z* 560.1839 $[M]^+$ (calcd for $C_{35}H_{28}O_7$, 560.1835).

Cell Culture and Induction of 3T3-L1 Adipocytes. 3T3-L1 cells were purchased from American Type Culture Collection (ATCC, Manassas, VA, USA) and grown in DMEM with 10% FCS. To induce differentiation, 3T3-L1 preadipocytes were cultured until confluence was reached (0 day), and the culture medium was replaced with a fresh induction medium containing 5 μg/mL insulin, 0.5 mM 3-isobutyl-1-methylxanthine (IBMX), and 1 μM dexamethasone (DEX) in DMEM with 10% FBS for 2 days. The medium was then replaced with a differentiation medium containing 5 μg/mL insulin and DMEM with 10% FBS every 2 days for up to 8 days until the cells were harvested.

Cell Viability Assay. The viability of cultured cells was assessed using an MTT assay. In brief, 3T3-L1 (1×10^4 cells/well) cells seeded in 96-well plates were treated with various concentrations of samples for 48 h. Then, MTT solution (1 mg/mL) was added to each well, and the cells were incubated at 37 °C for 1 h. Finally, DMSO was added to dissolve the formazan crystals. Absorbance was measured at 540 nm using a spectrophotometer (Immuno Mini NJ-2300, Japan).

Adipocyte-Based Measurement of 2-NBDG Uptake. 3T3-L1 adipocytes grown in black 96-well plates were incubated with each sample for 24 h at 37 °C in a 5% CO_2 atmosphere. Subsequently, 250 μM 2-NBDG (dissolved in PBS with 1% BSA) was added to the cells

DOI: 10.1021/np5005856
J. Nat. Prod. 2015, 78, 34−42

and incubated for a further 30 min. After incubation, cells were washed two times with PBS to remove excess fluorescence in the wells. Then, fluorescence retained by the cells was measured using a PerkinElmer Victor3 V 1420 multilabel plate counter at an excitation and emission wavelength of 485 and 535 nm, respectively.

PTP1B Inhibitory Assay. Protein tyrosine phosphatase 1B (human recombinant) was purchased from Biomol International LP, Plymouth Meeting, PA, USA, and the inhibitory activities of the tested samples were evaluated using *p*-nitrophenyl phosphate (*p*-NPP) as substrate.[26] To each well (final volume 110 μL) were added 2 mM *p*-NPP and PTP1B in a buffer containing 50 mM citrate (pH 6.0), 0.1 M NaCl, 1 mM EDTA, and 1 mM dithiotheritol (DTT), with or without sample. The plate was preincubated at 37 °C for 10 min, and then 50 μL of *p*-NPP in buffer was added. Following incubation at 20 °C for 20 min, the reaction was terminated with the addition of 10 M NaOH. The amount of *p*-nitrophenyl produced after enzymatic dephosphorylation was estimated by measuring the absorbance at 405 nm using a VERSA Max microplate reader (Molecular Devices, Sunnyvale, CA, USA). The nonenzymatic hydrolysis of 2 mM *p*-NPP was corrected by measuring the increase in absorbance at 405 nm obtained in the absence of PTP1B enzyme. The inhibition (%) was calculated as $(A_c - A_s)/A_c \times 100\%$, where A_c is the absorbance of the control and A_s, the absorbance of the sample. Ursolic acid was used as positive control.

Statistical Analysis. Data are represented as means of triplicate assays ± SD. For statistical analysis of the data for single comparison, the significance between means was determined by the Student *t* test; $^*p < 0.05$, $^{**}p < 0.01$, and $^{***}p < 0.001$ compared with the control.

■ ASSOCIATED CONTENT

Supporting Information

1D NMR spectra of compounds **1**−**5**, 2D NMR spectra of compounds **2**, **4**, and **5**, HPLC profiles and UV−vis spectra of compounds **1**−**5**, and cytotoxic effects of compounds **1**−**5** on 3T3-L1 adipocyte cells are available free of charge via the Internet at http://pubs.acs.org.

■ AUTHOR INFORMATION

Corresponding Author

*(M.-H. Woo) Tel/Fax: +82-53-850-3620. E-mail: woomh@cu.ac.kr.

Notes

The authors declare no competing financial interest.

■ ACKNOWLEDGMENTS

This work was supported as a Basic Science Research Program through the National Research Foundation of Korea (NRF), funded by the Ministry of Education, Science and Technology (no. 2010-0010549), and the BK 21 Plus Program of the Ministry of Education, Science and Technology, Korea. We are grateful to the Korea Basic Science Institute (KBSI) for mass spectrometric measurements.

■ REFERENCES

(1) Pereira, D. F.; Cazarolli, L. H.; Lavado, C.; Mengatto, V.; Figueiredo, M. S. R. B.; Guedes, A.; Pizzolatti, M. G.; Silva, F. R. M. B. *Nutrition* **2011**, *27*, 1161−1167.

(2) Gershell, L. *Nat. Rev. Drug Discovery* **2005**, *4*, 367−368.

(3) (a) Marx, J. *Science* **2002**, *296*, 686−689. (b) American Diabetes Association.. *Diabetes Care* **2013**, *36*, 1033−1046.

(4) Kumar, S.; Narwal, S.; Kumar, V.; Prakash, O. *Pharmacogn. Rev.* **2011**, *5*, 19−29.

(5) (a) Umpierrez, G. E.; Palacio, A.; Smiley, D. *Am. J. Med.* **2007**, *120*, 563−567. (b) Nishide, M.; Yoshikawa, Y.; Yoshikawa, E. U.; Matsumoto, K.; Sakurai, H.; Kajiwara, N. M. *Chem. Pharm. Bull.* **2008**, *56*, 1181−1183.

(6) Zhang, B.; Salituro, G.; Szalkowski, D.; Li, Z.; Zhang, Y.; Royo, I.; Vilella, D.; Diez, M. T.; Pelaez, F.; Ruby, C.; Kendall, R. L.; Mao, X.; Griffin, P.; Calaycay, J.; Zierath, J. R.; Heck, J. V.; Smith, R. G.; Möller, D. E. *Science* **1999**, *284*, 974−977.

(7) (a) Li, W. L.; Zheng, H. C.; Bukuru, J.; De Kimpe, N. *J. Ethnopharmacol.* **2004**, *92*, 1−21. (b) Malviya, N.; Jain, S.; Malviya, S. *Acta Polym. Pharm.* **2010**, *67*, 113−118. (c) Barros, L. F.; Young, M.; Saklatvala, J.; Baldwin, S. A. *J. Physiol.* **1997**, *504*, 517−525.

(8) Möller, D. E. *Nature* **2001**, *414*, 821−827.

(9) Johnson, T. O.; Ermolieff, J.; Jirousek, M. R. *Nat. Rev. Drug Discovery* **2002**, *1*, 696−709.

(10) Zhang, Z. Y.; Lee, S. Y. *Expert Opin. Investig. Drugs* **2003**, *12*, 223−233.

(11) Zhang, S.; Zhang, Z. Y. *Drug Discovery Today* **2007**, *12*, 373−381.

(12) Little, D. P.; Moran, R. C.; Brenner, E. D.; Stevenson, D. W. *Genome* **2007**, *50*, 351−356.

(13) Yang, S. Z.; Flaws, B. *The Divine Farmer's Material Medica: A Translation of the Shen Nong Ben Cao Jing*; Blue Poppy Press: Boulder, CO, 1998.

(14) Miao, N.; Tao, H.; Tong, C.; Xuan, H.; Zhamg, G. *Zhongguo Zhong Yao Za Zhi* **1996**, *21*, 493−495.

(15) (a) Bi, Y. F.; Zheng, X. K.; Feng, W. S.; Shi, S. P. *Acta Pharm. Sin.* **2004**, *39*, 41−45. (b) Wang, Y. Z.; Chen, H.; Zheng, X. K.; Feng, W. S. *Chin. Chem. Lett.* **2007**, *18*, 1224−1226. (c) Zheng, X. K.; Li, K. K.; Wang, Y. Z.; Feng, W. S. *Chin. Chem. Lett.* **2008**, *19*, 79−81.

(16) (a) Zhang, L. P.; Liang, Y. M.; Wei, X. C.; Cheng, D. L. *J. Org. Chem.* **2007**, *72*, 3921−3924. (b) Zhang, G. G.; Jing, Y.; Zhang, H. M.; Ma, E. L.; Guan, J.; Xue, F. N.; Liu, H. X.; Sun, X. Y. *Planta Med.* **2012**, *78*, 390−392. (c) Yang, C.; Shao, Y.; Li, K.; Xia, W. *Beilstein J. Org. Chem.* **2012**, *8*, 1884−1889.

(17) (a) Cheng, X. L.; Ma, S. C.; Yu, J. D.; Yang, S. Y.; Xiao, X. Y.; Hu, J. Y.; Lu, Y.; Shwa, P. C.; But, P. P. H.; Lin, R. C. *Chem. Pharm. Bull.* **2008**, *56*, 982−984. (b) Kirste, B.; Harrer, W.; Kurreck, H.; Schubert, K.; Bauer, H.; Gierke, W. *J. Am. Chem. Soc.* **1981**, *103*, 6280−6286.

(18) (a) Xu, K. P.; Zou, H.; Tan, Q.; Li, F. S.; Liu, J. F.; Xiang, H. L.; Zou, Z. X.; Long, H. P.; Li, Y. J.; Tan, G. S. *J. Asian Nat. Prod. Res.* **2011**, *13*, 93−96. (b) Xu, K. P.; Zou, H.; Liu, G. R.; Long, H. P.; Li, J.; Li, F. S. *J. Asian Nat. Prod. Res.* **2011**, *13*, 1051−1055. (c) Tan, G. S.; Xu, K. P.; Li, F. S.; Wang, C. J.; Li, T. Y.; Hu, C. P. *J. Asian Nat. Prod. Res.* **2011**, *11*, 1001−1004. (d) Cao, Y.; Chen, J. J.; Tan, N. H.; Oberer, L.; Wagner, T.; Wu, Y. P.; Zeng, G. Z.; Yan, H.; Wang, Q. *Bioorg. Med. Chem. Lett.* **2010**, *20*, 2456−2460. (e) Cao, Y.; Chen, J. J.; Tan, N. H.; Wu, Y. P.; Yang, J.; Wang, Q. *Magn. Reson. Chem.* **2010**, *48*, 656−659.

(19) Croteau, R.; Ketchum, R. E.; Long, R. M.; Kaspera, R.; Wildung, M. R. *Phytochem. Rev.* **2006**, *5*, 75−97.

(20) Barnett, A. H. *Vasc. Health Risk Manag.* **2006**, *2*, 59−67.

(21) Shrestha, S.; Bhattarai, B. R.; Cho, H.; Choi, J. K.; Cho, H. *Bioorg. Med. Chem. Lett.* **2007**, *17*, 2728−2730.

(22) (a) Kim, W. H.; Lee, J.; Jung, D. W.; Williams, D. R. *Sensors* **2012**, *12*, 5005−5027. (b) Lee, J.; Jung, D. W.; Kim, W. H.; Um, J. I.; Yim, S. H.; Oh, W. K.; Williams, D. R. *ACS Chem. Biol.* **2013**, *8*, 1803−1814.

(23) (a) Zou, C.; Wang, Y.; Shen, Z. *J. Biochem. Biophys. Methods* **2005**, *64*, 207−215. (b) Nitin, N.; Carlson, A. L.; Muldoon, T.; El-Naggar, A. K.; Gillenwater, A.; Richards-Kortum, R. *Int. J. Cancer* **2009**, *124*, 2634−2642. (c) Jung, D. W.; Ha, H. H.; Zheng, X.; Chang, Y. T.; Williams, D. R. *Mol. BioSyst.* **2011**, *7*, 346−358. (d) Millon, S. R.; Ostrander, J. H.; Brown, J. Q.; Raheja, A.; Seewaldt, V. L.; Ramanujam, N. *Breast Cancer Res. Treat.* **2011**, *126*, 55−62.

(24) (a) Huang, S.; Czech, M. P. *Cell Metab.* **2007**, *5*, 237−252. (b) Kozma, S. C.; Thomas, G. *Bioessays* **2002**, *24*, 65−71. (c) Chang, L.; Chiang, S. H.; Saltiel, A. R. *Mol. Med.* **2004**, *10*, 65−71.

(25) (a) Cheng, A.; Uetani, N.; Simoncic, P. D.; Chaubey, V. P.; Lee-Loy, A.; McGlade, C. J.; Kennedy, B. P.; Tremblay, M. L. *Dev. Cell* **2002**, *2*, 497−503. (b) Elchebly, M.; Payette, P.; Michaliszyn, E.; Cromlish, W.; Collins, S.; Loy, A. L.; Normandin, D.; Cheng, A.;

DOI: 10.1021/np5005856
J. Nat. Prod. 2015, 78, 34−42

Himms-Hagen, J.; Chan, C. C.; Ramachandran, C.; Gresser, M. J.; Tremblay, M. L.; Kennedy, B. P. *Science* **1999**, *283*, 1544−1548.
(26) Na, M.; Cui, L.; Min, B. S.; Bae, K.; Yoo, J. K.; Kim, B. Y.; Oh, W. K.; Ahn, J. S. *Bioorg. Med. Chem. Lett.* **2006**, *16*, 3273−3276.
(27) Athare, C. L.; Singh, N.; Upasani, C. D. *World J. Pharm. Res.* **2014**, *3*, 2232−2247.
(28) (a) Zheng, X. K.; Zhang, L.; Wang, W. W.; Wu, Y. Y.; Zhang, Q. B.; Feng, W. S. *J. Ethnopharmacol.* **2011**, *137*, 662−668. (b) Zheng, X. K.; Li, Y. J.; Zhang, L.; Feng, W. S.; Zhang, X. *J. Ethnopharmacol.* **2011**, *133*, 531−537. (c) Shi, S. P.; Wang, Y. Z.; Zheng, X. K.; Feng, W. S.; Tu, P. F. *Biochem. Syst. Ecol.* **2012**, *45*, 151−154.

DOI: 10.1021/np5005856
J. Nat. Prod. 2015, 78, 34−42